Magnetoresistance behaviour of $La_{1-x}Ca_xMnO_3$ compounds



1996 J. Phys.: Condens. Matter 8 5393

(http://iopscience.iop.org/0953-8984/8/29/014)

J. Phys.: Condens. Matter **8** (1996) 5393–5400. Printed in the UK

# Magnetoresistance behaviour of $La_{1-x}Ca_xMnO_3$ compounds

G H Rao, J R Sun, Y Z Sun, Y L Zhang and J K Liang

Institute of Physics, Chinese Academy of Sciences, PO Box 603, Beijing 100080, People's Republic of China

Received 17 November 1995, in final form 23 January 1996

**Abstract.** The magnetoresistance behaviour of $La_{1-x}Ca_xMnO_3$ has been systematically investigated between 77 and 300 K; it depends strongly upon the $Mn^{4+}$ content in the sample. For $0 \leqslant x_{Mn^{4+}} \leqslant 0.1$ and $0.5 \leqslant x_{Mn^{4+}} \leqslant 0.71$, the samples exhibit antiferromagnetic and semiconducting characters, and the resistance obeys Mott's law: $\ln R \propto 1/T^{1/4}$. For $0.25 \leqslant x_{Mn^{4+}} \leqslant 0.375$, the sample is ferromagnetic and metallic in the temperature range below $T_c$. A negative magnetoresistance as large as 50% was observed in a bulk sample with $x_{Mn^{4+}} = 0.27$ in a field of 1 T. In the two phase ranges ($0.1 < x_{Mn^{4+}} < 0.25$ and $0.375 < x_{Mn^{4+}} < 0.5$), antiferromagnetic domains and ferromagnetic domains are assumed to distribute randomly in *one* crystallographic lattice, and the effective-medium theory provides a satisfactory interpretation for the resistance behaviour of the samples.

## 1. Introduction

The discovery of high-temperature superconductivity has renewed interest in mixed-valence cubic perovskite compounds. Recently, large negative magnetoresistance (GMR) effects have been observed in films of perovskite of the general formula $R_{1-x}A_xMnO_3$ (R = La or Nd, A = Ca, Sr or Ba) [1–3], which are considerably larger than the GMR effects observed in magnetic multilayers and alloys. Most previous studies on the GMR in $R_{1-x}A_xMnO_3$ focused on a particular composition around $x = 1/3$, at which the double-exchange interaction between $Mn^{3+}$ and $Mn^{4+}$ ions in these compounds is believed to be optimal and responsible for the occurrence of both ferromagnetism and metallic conductivity [4, 5]. The GMR effect in these films could be strongly influenced by the preparation conditions [1], which essentially change the $Mn^{4+}$ content in the sample in addition to affecting the epitaxy, defect density, chemical homogenization and substrate–film interactions. According to the theory of semicovalent exchange [6], the $Mn^{4+}$ content in $R_{1-x}A_xMnO_3$ plays a crucial role in controlling the magnetic lattice, the crystallographic lattice and the electrical resistivity of the compounds. In this paper, we report our systematic investigation of the magnetoresistance behaviour of the bulk samples of $La_{1-x}Ca_xMnO_3$ with different $Mn^{4+}$ contents, which should be helpful for understanding the mechanism of the GMR effect in these perovskites and for optimizing the preparation conditions.

## 2. Experimental procedures

$La_{1-x}Ca_xMnO_3$ ($x = 0$–0.6) samples were prepared by calcining stoichiometric mixtures of $La_2O_3$, $MnCO_3$ and $CaCO_3$ at 1123 K for 24 h. The powder thus obtained was

0953-8984/96/295393+08$19.50  

**Table 1.** The $Mn^{4+}$ content and the Curie temperature in $La_{1-x}Ca_xMnO_3$.

| $x$ | $x_{Mn^{4+}}$ [a] | $T_c$ (K)[a] | $x_{Mn^{4+}}$ [b] | $T_c$ (K)[b] | $x_{Mn^{4+}}$ [c] | $T_c$ (K)[c] |
|---|---|---|---|---|---|---|
| 0.0 | 0.23 | 254 | 0.24 | 257 | 0.10 | — |
| 0.05 | 0.28 | 266 | 0.25 | 261 | 0.12 | — |
| 0.10 | 0.27 | 250 | 0.34 | 270 | 0.14 | 182 |
| 0.15 | 0.28 | 251 | 0.35 | 270 | 0.18 | 186 |
| 0.20 | 0.29 | 264 | 0.31 | 260 | 0.22 | 221 |
| 0.25 | 0.32 | 266 | 0.38 | 278 | 0.33 | 274 |
| 0.30 | 0.36 | 272 | 0.42 | 277 | 0.30 | 261 |
| 0.35 | 0.40 | 276 | 0.47 | 274 | 0.43 | 272 |
| 0.40 | 0.42 | 274 | 0.45 | 273 | 0.44 | 273 |
| 0.45 | 0.48 | 261 | 0.49 | 270 | 0.46 | 275 |

[a]Samples sintered in air.
[b]Samples sintered in $O_2$.
[c]Samples sintered in $N_2$.

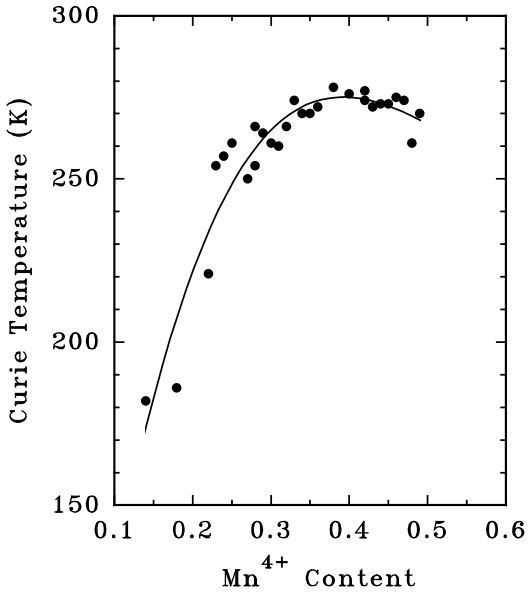


**Figure 1.** The dependence of the Curie temperature on the $Mn^{4+}$ content in $La_{1-x}Ca_xMnO_3$.

ground, pelletized and sintered at 1373 K for another 24–72 h, then furnace cooled to room temperature. The phase purity and crystal structure were checked by using a four-layer monochromatic focusing Guinier de Wolff camera and Cu K$\alpha$ radiation. The $Mn^{4+}$ content in the sample was determined by iodometric titration and is believed to be reliable to within about 5%. The low-field ac susceptibility between 77 and 300 K was measured by means of a sensitive mutual inductance method with a frequency of 320 Hz. The resistance measurements were carried out on sintered pellets by the standard four-probe method in a field of zero or 1 T. The magnitude of the magnetoresistance is defined as $\Delta R/R = [R(H) - R(0)]/R(0)$, where $R(H)$ and $R(0)$ are the resistances in a field of 1 T and in zero field, respectively.

## 3. Experimental results

X-ray diffraction and ac susceptibility measurements revealed that a single phase was obtained in $La_{1-x}Ca_xMnO_3$ with $x = 0 - 0.6$. Table 1 presents the measured $Mn^{4+}$ content in the sample and the Curie temperature. The measured $Mn^{4+}$ content, $x_{Mn^{4+}}$, in the sample sintered in air was considerably larger than the nominal Ca content, $x$, at lower $x$-values, and was close to the nominal Ca content at higher $x$-values (>45%). Postannealing samples in $O_2$ (or $N_2$) at 1273 K for 24 h increased (or decreased) the $Mn^{4+}$ content in the samples, especially in those with lower $x$-values. A rhombohedral structure, which belongs to the distorted perovskite structure, was observed in the samples with $x_{Mn^{4+}} < 0.2$, and a cubic perovskite structure was obtained in the samples with $x_{Mn^{4+}} \geqslant 0.2$. The present XRD analysis is consistent with a previous report [7].

Figure 1 shows the dependence of the Curie temperature, $T_c$, on the $Mn^{4+}$ content in the sample. A maximum at around $x_{Mn^{4+}} = 0.38$ is present. For $x_{Mn^{4+}} < 0.38$, $T_c$ increases with $Mn^{4+}$ content, while for $x_{Mn^{4+}} > 0.38$, $T_c$ decreases slightly with $x_{Mn^{4+}}$. The present result agrees well with the neutron diffraction experiment [8].

Typical temperature dependences of the resistivity and MR effect are shown in figure 2. The downwards arrows indicate the magnetic transition temperatures determined by ac susceptibility measurements. The temperature dependence of the resistivity is strongly influenced by the $Mn^{4+}$ content in the sample. For $0 \leqslant x_{Mn^{4+}} \leqslant 0.1$ and $x_{Mn^{4+}} \geqslant 0.5$, the samples exhibit insulator or semiconductor characters (figure 2(a)). For $0.25 \leqslant x_{Mn^{4+}} \leqslant 0.375$, both the resistance and MR effect have sharp peaks at around the Curie temperature, $T_c$ (figure 2(c)). A MR effect with $|\Delta R/R| = 50\%$ was observed in the sample with $x_{Mn^{4+}} = 0.27$ in a field of 1 T. For $0.1 < x_{Mn^{4+}} < 0.25$ and $0.375 < x_{Mn^{4+}} < 0.5$, the resistance exhibits two peaks (figure 2(b)): a sharp one at around $T_c$ and a broad one below $T_c$. As the $Mn^{4+}$ content deviates from 0.3, the optimal value for the double-exchange interaction, the height of the broad peak increases and the peak shifts to lower temperature (figure 3).

Figure 4 shows the temperature dependence of the low-field ac susceptibility of the sample with different $Mn^{4+}$ contents. There is a close correlation between the magnetic properties and the resistivity behaviour, as discussed below.

## 4. Discussions

Based on the theory of semicovalent exchange and with the hypothesis of covalent and semicovalent bonding between the oxygen and the manganese ions plus the mechanism of double exchange, Goodenough qualitatively predicted the magnetic phase diagram of the perovskite-type manganate $La_{1-x}A_xMnO_3$ (A = Ca, Sr, Ba) [6]. The prediction coincided well with the findings from neutron diffraction and x-ray diffraction as well as the magnetic saturation data [8]. It is striking that the resistivity and MR behaviours in $La_{1-x}Ca_xMnO_3$ observed in the present investigation closely mimic the predicted magnetic phase diagram. The behaviours shown in figures 1(a)–1(c) correspond to phase regions $\alpha$ (or $\gamma$), $\alpha + \beta$ (or $\beta + \gamma$) and $\beta$, respectively.

Phase $\alpha$ ($0 \leqslant x_{Mn^{4+}} \leqslant 0.1$) is the terminal solid solution of $LaMnO_3$ and is antiferromagnetic with high resistivity, while the parent insulator $LaMnO_3$ is a Mott insulator due to strong correlation of the $e_g$ electrons [9]. Phase $\gamma$ ($0.5 \leqslant x_{Mn^{4+}} \leqslant 0.71$) is an ordered phase and is also antiferromagnetic with relatively high resistivity. Magnetoresistance in these two phases is negligible in a field of 1 T. However, the resistances of both phases obey well Mott's law: $\ln \rho \propto 1/T^{1/4}$, in the temperature range between 77 and 300 K

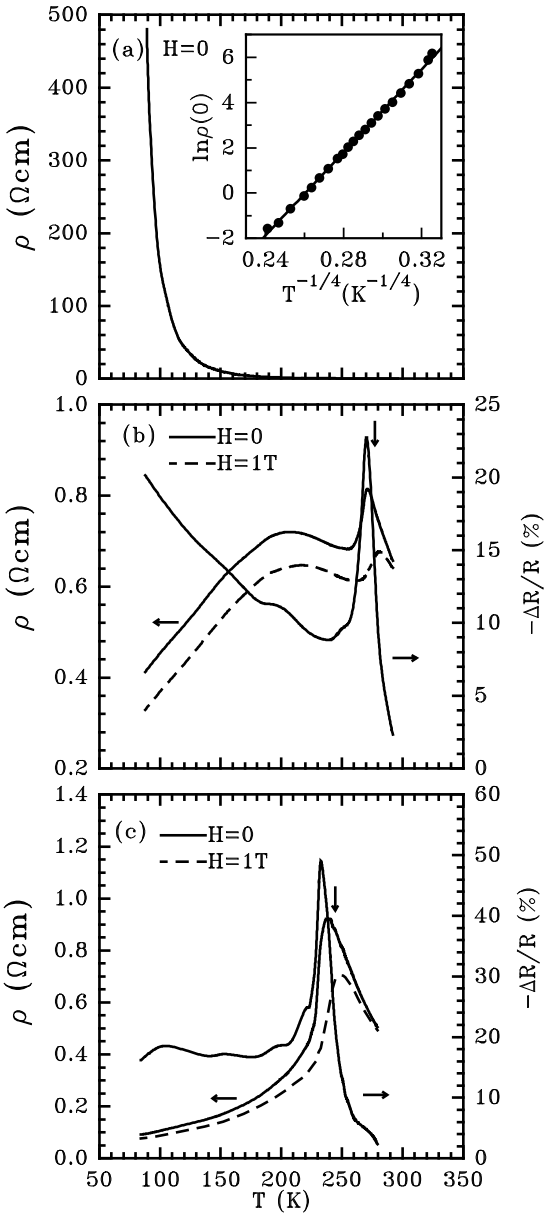


**Figure 2.** Typical magnetoresistance behaviour of $La_{1-x}Ca_xMnO_3$ with different $Mn^{4+}$ contents. Magnetic transition temperatures are marked by downwards arrows. (a) $x_{Mn^{4+}} = 0.60$; (b) $x_{Mn^{4+}} = 0.40$; (c) $x_{Mn^{4+}} = 0.27$.

(see the inset in figure 2(a)), which indicates that the conductivity is dominated by the variable-range hopping (VRH) process of the carriers. In fact, the competing interactions: covalent, semicovalent and double exchange [6], existing in $La_{1-x}Ca_xMnO_3$ give rise to a strongly perturbed spin lattice, which in combination with the narrow conduction band can lead to the localization of states and the formation of polarons, as originally suggested by Mott (see [10]).

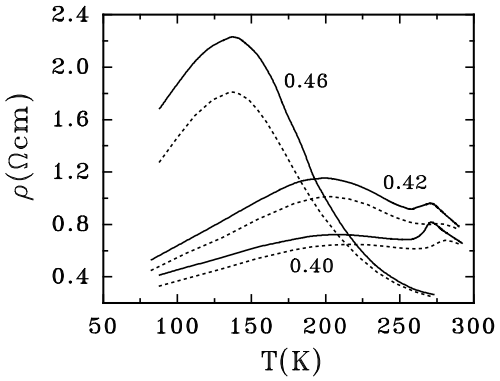


**Figure 3.** The resistivity behaviour of $La_{1-x}Ca_xMnO_3$ in the two-phase region. Solid and dotted lines represent the resistivities in fields of zero and 1 T, respectively. The $Mn^{4+}$ content is indicated by the numbers.

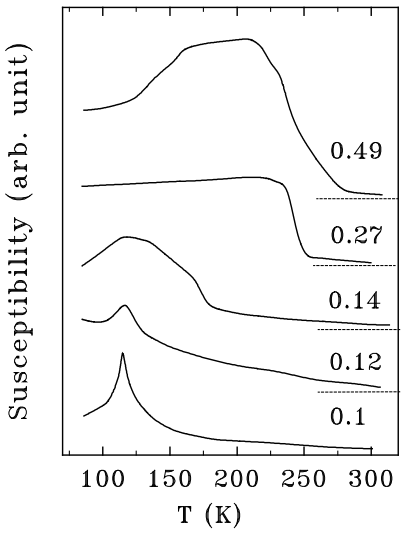


**Figure 4.** Temperature dependences of the low-field ac susceptibility of the samples with different $Mn^{4+}$ contents. The $Mn^{4+}$ contents are indicated by the numbers. The dashed line represents the base-line for $\chi_{ac}$.

The magnetoresistance behaviour of phase $\beta$ ($0.25 \leqslant x_{Mn^{4+}} \leqslant 0.375$) has been extensively investigated recently [1–3, 9, 11]. In phase $\beta$, $Mn^{3+}$ and $Mn^{4+}$ are randomly distributed. The double-exchange interaction between $Mn^{3+}$ and $Mn^{4+}$ gives rise to both ferromagnetism and metallic conductivity of phase $\beta$ [4–6]. As the temperature approaches $T_c$, the increase of resistance results from the increase in the carrier scattering by thermal spin fluctuation, since the double-exchange theory indicates that the effective electron (hole) transfer ($\overline{t_{ij}}$) between the neighbouring sites depends on the relative angle ($\Delta\Theta_{ij}$) of the local spins as $\overline{t_{ij}} = t_{ij}\cos(\Delta\Theta_{ij}/2)$. An intuitive view on the MR effect is that the magnetic field tends to align the local spins, and the forcedly spin-polarized conduction electron suffers less from the scattering by local spins and becomes more itinerant. Above the Curie temperature, much of the behaviour of the resistivity data is indicative of a hopping

conduction of magnetic polarons [12], i.e. the spin of a conducting electron induces a local distortion of the spin lattice and moves on surrounded by this spin polarization. Experimental evidence for magnetic polarons above $T_c$ was found from spin-polarized neutron scattering for the similar compound $Nd_{0.5}Pb_{0.5}MnO_3$ [12] and from the magnetovolume effect for $(La_{3/4}Tb_{1/4})_{2/3}Ca_{1/3}MnO_3$ [13]. An applied field will increase the ferromagnetic order in a crystal, so magnetic polaron formation will be inhibited and a very prominent MR effect will occur at around $T_c$.

In the two-phase range $\alpha + \beta$ ($0.1 < x_{Mn^{4+}} < 0.25$), $T_c$ increases with $x_{Mn^{4+}}$, while in the two-phase range $\beta + \gamma$ ($0.375 < x_{Mn^{4+}} < 0.5$), $T_c$ decreases as $x_{Mn^{4+}}$ increases. Moreover, the two-phase character in these two-phase ranges could only be detected by neutron diffraction instead of x-ray diffraction [6]. These observations indicate that the two-phase character is not a simple mechanical mixture of $\alpha$ and $\beta$ (or $\beta$ and $\gamma$), but a distribution of antiferromagnetic (AF) domains and ferromagnetic (F) domains in *one* crystallographic lattice. Taking into account the temperature dependences of the resistances in phases $\alpha, \beta$ and $\gamma$ (figure 2) and assuming that the AF domains and F domains are distributed randomly in the lattice, we can use effective-medium theory [14, 15] to describe the resistance of the samples in the two-phase region:

$$\rho = \frac{4\rho_1\rho_2}{[(3p-1)\rho_1 + (2-3p)\rho_2] + \sqrt{[(3p-1)\rho_1 + (2-3p)\rho_2]^2 + 8\rho_1\rho_2}} \tag{1}$$

where $p$ is the volume fraction of phase $\beta$, $\rho_1$ is the resistivity of phase $\alpha$ or $\gamma$, which decreases with temperature after Mott's VRH law: $\rho_1 = a_1 e^{(T_0/T)^{1/4}}$, while $\rho_2$ is the resistivity of phase $\beta$, which increases with temperature below $T_c$. According to equation (1), the opposite temperature dependences of $\rho_1$ and $\rho_2$ would give rise to the broad peak far below $T_c$ as shown in figure 2(b).

To model the resistivity data of the sample in the two-phase range by using equation (1), it is necessary to know the analytical expressions for the temperature dependence of $\rho_1$ and $\rho_2$. Unfortunately, there is no report of such a expression for phase $\beta$, partially due to the complex conduction mechanism around $T_c$. According to the double-exchange theory, the resistivity of phase $\beta$ can be approximated as $\rho_2 = a_2 + b_2 T$, at a temperature far below $T_c$ [4]. As shown in figure 2(c), the resistivity of phase $\beta$ increases with temperature and deviates from the linear metallic behaviour strikingly as the temperature approaches the Curie temperature. However, if the resistivity peak around $T_c$ is very small, it is expected that the linear metallic resistivity: $\rho_2 = a_2 + b_2 T$, will provide a good approximation for the resistivity of phase $\beta$.

Among our experimental data, resistivity data fulfilling above condition are obtained exclusively in a very limited number of samples. Figure 5 shows the resistivity data for the sample with $x_{Mn^{4+}} = 0.46$. The solid lines indicate that equation (1) gives a satisfactory fitting to the measured temperature dependences with $a_1 = (1.48 \pm 0.66) \times 10^{-18}$ Ω cm, $T_0 = (7.63 \pm 0.30) \times 10^8$ K, $a_2 = (5.25 \pm 0.47) \times 10^{-3}$ Ω cm, $b_2 = (1.34 \pm 0.04) \times 10^{-4}$ Ω cm $K^{-1}$ and $p = 0.340 \pm 0.009$ for $\rho(0)$. $a_1 = (7.29 \pm 1.54) \times 10^{-17}$ Ω cm, $T_0 = (5.13 \pm 0.11) \times 10^8$ K, $a_2 = (3.25 \pm 2.39) \times 10^{-4}$ Ω cm, $b_2 = (1.43 \pm 0.02) \times 10^{-4}$ Ω cm $K^{-1}$ and $p = 0.340 \pm 0.008$ for $\rho(H)$. The value of $p$ obtained is consistent with the measured $Mn^{4+}$ content in the sample and the magnetic phase diagram according to the lever rule. When an external field is applied, $a_2$ (the residue resistance of phase $\beta$) and $T_0$ decrease, while $b_2$ slightly increases. The value of $T_0$ obtained is an order of magnitude larger than that of pure phase $\gamma$ ($T_0 = (7.14 \pm 0.22) \times 10^7$ K from fitting the data in figure 1(a)), which seems to indicate that the randomly distributing F domains make some contribution to the random potential in the lattice. Assuming that the density of states at the Fermi level is of the order of $10^{19}$, the

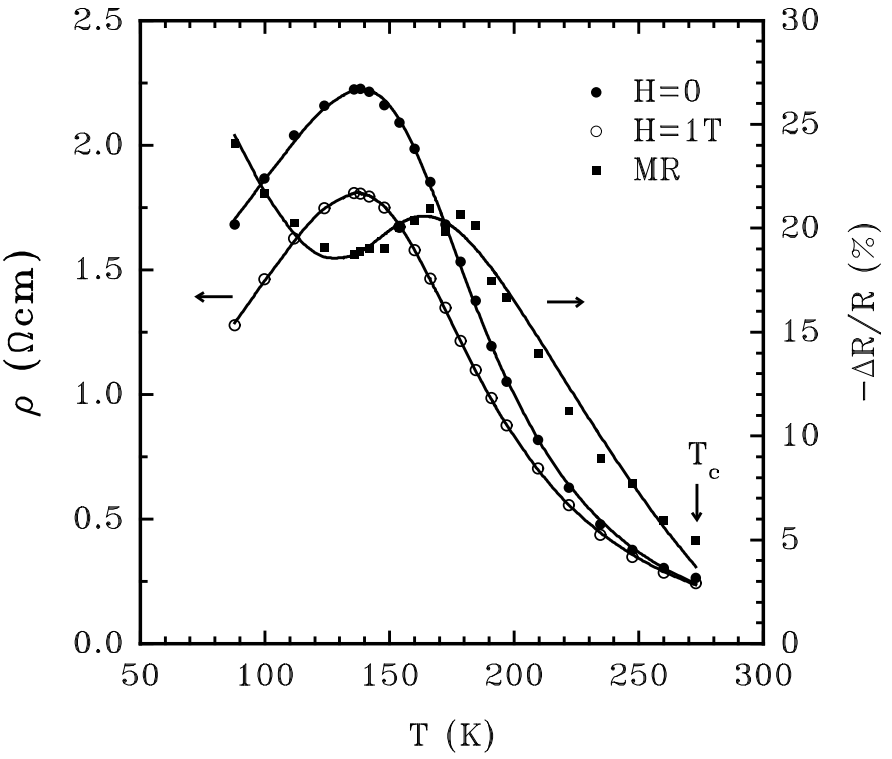


**Figure 5.** The magnetoresistance behaviour of $La_{1-x}Ca_xMnO_3$ with $x_{Mn^{4+}} = 0.46$. The symbols show some of the data read from measured $R$–$T$ curves. The solid MR–$T$ curve is derived from the calculated $R(0)$ and $R(H)$ instead of from fitting the MR data.

coefficient of the exponential decay of the localized states, $\alpha$, is estimated to be $3\times10^7$ cm$^{-1}$, which is within the general estimation range [16], and the most probable hopping distance $r^* \approx 60$ Å at 100 K, which is about 16 times the distance between two nearest $Mn^{3+}/Mn^{4+}$ ions in the crystal structure (∼3.89 Å [1]). Therefore, the satisfactory fitting of equation (1) to the measured resistance data and the meaningful parameters obtained seem to justify our proposed model for the resistance behaviour of the samples in the two-phase ranges, especially for the existence of the broad peak far below $T_c$.

To examine the dependence on $Mn^{4+}$ content of the height and position of the broad peak, the variation of $Mn^{4+}$ content is assumed to change $p$-value only within the first-order approximation; thus it is easy to derive from equation (1) and the above-obtained parameters that the peak height decreases and the peak position shifts to higher temperature as the $Mn^{4+}$ content decreases, which is consistent with the present observation (figure 3).

The resistivity behaviour in the two-phase region is characterized by the existence of a broad resistivity peak far below $T_c$, which is less reported in previous publications. Neumeier *et al* observed that the broad peak could be induced by the application of an external pressure in $La_{1-x}Ca_xMnO_3$, and attributed this feature to a magnetic transition from a ferromagnetic state to a canted ferromagnetic state [17]. The effective-medium theory provides an alternative interpretation and is actually based upon a magnetic inhomogeneity in the sample [18]. Neutron diffraction favours the magnetic inhomogeneity model due to the presence of the phase boundary [8, 19]. In the two-phase region, the MR behaviour of

the AF phase might be different from that of the pure AF phase, owing to the influence of the coexisting F phase and the size effect of the AF domain. When the AF domain is small and surrounded by F domains, an appreciable number of carriers near the AF domain boundary have a high probability of being delocalized and this gives rise to a noticeable MR effect.

As shown in figure 4, the ac susceptibility of the sample close to the $\beta+\gamma/\gamma$ boundary exhibits another magnetic transition below $T_c$, which probably indicates the formation of spin glass [18]. Hysteresis in the temperature dependence of the resistivity was observed on cooling and heating. It was also found that when the external field was switched off, the resistivity recovered the zero-field value very sluggishly. The resistivity and MR behaviours of these samples are under further investigation.

## 5. Summary

In summary, the magnetoresistance behaviour of $La_{1-x}Ca_xMnO_3$ ($0 \leqslant x \leqslant 0.6$) was systematically investigated. The magnetoresistance behaviour depends strongly on the $Mn^{4+}$ content in the sample and closely mimics the magnetic phase diagram predicted based upon the theory of semicovalent exchange. The phase $\beta$ ($0.25 \leqslant x_{Mn^{4+}} \leqslant 0.375$) is ferromagnetic and metallic in the temperature range below $T_c$. The conduction in the antiferromagnetic phases $\alpha$ ($0 \leqslant x_{Mn^{4+}} \leqslant 0.1$) and $\gamma$ ($0.5 \leqslant x_{Mn^{4+}} \leqslant 0.71$) proceeds via variable-range hopping of carriers: $\ln R \propto 1/T^{1/4}$. In the two-phase ranges ($\alpha+\beta$ or $\beta+\gamma$), the effective-medium theory provides a satisfactory interpretation for the magnetoresistance behaviour of the samples. The present investigation should be helpful for understanding the mechanism of the MR effect in $R_{1-x}A_xMnO_3$ and for optimizing sample preparation conditions.

## References


[1] Jin S, Tiefel T H, McCormack M, Fastnacht R A, Ramesh R and Chen L H 1994 *Science* **264** 413
[2] Xiong G C, Li Q, Ju H L, Mao S N, Senapati L, Xi X X, Greene R L and Venkatesan T 1995 *Appl. Phys. Lett.* **66** 1427
[3] von Helmolt R, Wecker J, Holzapfel B, Schultz L and Samwer K 1993 *Phys. Rev. Lett.* **71** 2331
[4] Zener C 1951 *Phys. Rev.* **82** 403
[5] de Gennes P G 1960 *Phys. Rev.* **118** 141
[6] Goodenough J B 1955 *Phys. Rev.* **100** 564
[7] Mahesh R, Maheudiran R, Raychaudhuri A K and Rao C N R 1995 *J. Solid State Chem.* **114** 297
[8] Wollan E O and Koehler W C 1955 *Phys. Rev.* **100** 545
[9] Tokura Y, Urushibara A, Moritomo Y, Arimo T, Asamitsu A, Kido G and Furukawa N 1994 *J. Phys. Soc. Japan* **63** 3931
[10] Mott N F and Davis E A 1979 *Electronic Processes in Noncrystalline Materials* (Oxford: Clarendon)
[11] Furukawa N 1994 *J. Phys. Soc. Japan* **63** 3214
[12] Kusters R M, Singleton J, Keen D A, McGreevy R and Hayes W 1989 *Physica* B **155** 362
[13] De Teresa J M, Blasco J, Ibarra M R, García J, Marquina C, Algarabel P and del Moral A 1995 *Solid State Commun.* **96** 627
[14] Landauer R 1952 *J. Appl. Phys.* **23** 779
[15] Kirpatrick S 1971 *Phys. Rev. Lett.* **27** 1722
[16] Ambegaokar V, Halperin B I and Langer J S 1971 *Phys. Rev.* B **4** 2612
[17] Neumeier J J, Hundley M F, Thompson J D and Heffner R H 1995 *Phys. Rev.* B **52** R7006
[18] von Helmolt R, Wecker J, Lorenz T and Samwer K 1995 *Appl. Phys. Lett.* **67** 2093
[19] Jirák Z, Krupicka S, Simsa Z, Dlouhá M and Vratislav S 1985 *J. Magn. Magn. Mater.* **85** 153